한국콘크리트학회학술발표논문집
제 2 권 1 호 1990년 5월 19일

# 철근 콘크리트 部材의 히스테레틱 거동의 解析方法

Analytic Model for Hysteretic Behavior
of Reinforced Concrete Members

鄭 英 秀* 李 安 浩** C. Meyer ***
Chung, Young Soo Lee, An Ho

요 약

본 논문은 반복하중에 의한 콘크리트 부재거동에 대한 수학적인 해석방법에 관한 것으로서 철근콘크리트 부재의 Hysteretic 거동의 주요한 현상들인 강성저하, 강도저하 그리고 전단영향등의 수치해석 Model을 소개하였다. 그리고 본 해석 Model의 정확성 및 사용성등을 평가하기 위하여 RC 콘크리트 부재에 대한 수치 해석 예제를 제시하였다.

ABSTRACT

Mathematical hysteretic model has been developed to analytically reproduce the experimental hysteretic behavior of reinforced concrete members. This new model(2,3) is a rational simulation of the physical response characteristics of reinforced concrete member and better suitd for their nonlinear structural analysis, which are characterized by following important hysteretic behaviors: stiffness degradation, strength deterioation and shear effect. Numerical examples are presented to illustrate the capabilities between experimental and analytic response. The reproduction of hysteretic behavior of RC members appears be sufficiently accurate.

## 1 INTRODUCTION

The accurate prediction of the nonlinear behavior of reinforced concrete frames subjected to cyclic loading requires a mathematical model of reinforced concrete frame members. In this paper, the model of Meyer(8) is presented together with various enhancements. This model considers the effect of stiffness degradation, strength deterioration, shear and axial forces. A significant improvement is to reflect the strength deterioration, which is assumed to commence with the first exceedance of the yield moment and accelerates with each inelastic loading cycle in proportion to the amount by which the yield deformation is being exceeded. This model leads to analytical response predictions, which compare very well with experimental results and therefore can be considered to be better suited for dynamic response calculation than other previously proposed models.

## 2 Material Constitutive Laws

### 2.1 Concrete

It is well known that concrete exhibits different behavior in tension and compression. The tensile strength can be ignored under cyclic loading, because most of it is lost due to cracks caused by service loads. The stress-strain curve for plain concrete has been idealized by many researchers. Herein, Roufaiel and Meyer's refined curve(8) has been adopted with some minor modifications(2), Fig 1. It is fully described by specifying the following parameters, $f_{cu}=\alpha_c f'_c$, $f_{cy}=^3/_4 f_{cu}$, $\varepsilon_{cu}=\alpha_c \varepsilon_o$, $\varepsilon_{cy}=^5/_{12}\varepsilon_{cu}$, $\varepsilon_{cm}=\beta_c \varepsilon_{cu}$
where $f'_c$ is the uniaxial strength of concrete and $\varepsilon_o$ is the strain at $f'_c$, $\varepsilon_{cm}$ is the critical strain, at which the concrete cover can be observed to spall off, and which can be correlated to the onset of failure. Factors $\alpha_c = 1 + 10\rho''$ and $\beta_c = 2 + 600\rho''$ reflect the confining effect of transverse steel on concrete strength and critical strain, respec-

* 정회원 중앙대 토목과, 조교수 ** 중앙대 토목과 석사과정 *** 미국 Columbia대학, 부교수

tively; where

$\rho'' = \frac{2(b'' + d'')\ A_v}{b''\ d''\ s}$ = volumetric confinement steel ratio, b" and d" = width and depth of the confined core, $A_v$ = cross sectional area of transverse steel, s =spacing of transverse steel.

2.2 Tensile Reinforcing Steel

Stress-strain curves of steel bars used in reinforced concrete construction are typically idealized as bilinear curves, Fig2, characterized by Young's modulus. $E_s = f_{sy} / \varepsilon_{sy}$ for the elastic part and by the strain hardening parameter, $P_s = (1/E_s)*(f_{su} - f_{sy})/(\varepsilon_{su} - \varepsilon_{sy})$, for the inelastic part, where $f_{sy}$ = yield strength, $f_{su}$ = ultimate strength, $\varepsilon_{sy}$ = yield strain and $\varepsilon_{su}$ = ultimate strain. The unloading branch can be represented by a third linear branch with the negative slope, $-\overline{P}_s E_s = \gamma P_s E_s$. where can be determined from experimental test data for reinforcing steels. In this analysis, $\gamma = 2.0$ is used.

The descending branch of the stress-strain curve has a significance only for the material point undergoing failure. In order to facilitate our strength deterioration model for individual members as well as entire structures, it is important that the strain-softening branch of the material stress-strain law be included in the model. Thus, it is assumed that failure is initiated when $\varepsilon_s = \varepsilon_{su}$ and is complete when $\varepsilon_s = \alpha\ \varepsilon_{su}$(Fig2). The value of $\alpha$ is here assumed to be equal to 1.5.

2.3 Compressive Reinforcing Steel

The stress-strain curve for steel in compression is similar to that in tension, provided buckling is prevented. In the light of this restriction, it is very rare that steel bars in compression enter the strain hardening range. In reinforced concrete members, compression bars are restrained against buckling, as long as the concrete cover has not spalled off. The accurate determination of the buckling stress is very difficult. Herein, it is assumed that the bars cannot buckle before they are strained to the point at which the concrete cover spalls off.

**3 Primary Moment-Curvature Relationship.**

The primary moment-curvature curve relates moments to curvatures for monotonic loading. It can be idealized by three linear branches, Fig 3, one for the elastic loading part, one for the inelastic(strain hardening) loading part, and one for the unloading part. Once the stress-strain laws for steel and concrete are specified and the cross-sectional dimensions are known, it is relatively straightforward to compute the moment associated with any specified curvature. The $M - \phi$ curve is obtained by repeatedly computing the neutral axis, y, the curvature, $\phi$, and the bending moment, M, by increasing the concrete strain $\varepsilon_c$, or steel strain $\varepsilon_s$, from zero until any one of the possible failure modes is reached(2).

The definition proposed herein attempts to insert some objectivity by identifying limiting strains for the steel and concrete, after the exceedance of which the moment resisting capacity of a section is clearly deteriorating rapidly. Depending on the material parameters and sectional geometry, two important failure modes are considered as : 1) Flexural failure due to concrete crushing. Concrete crushes in compression when the compression strain reaches the value $\varepsilon_{cm}$. For this to happen in a properly under-reinforced section for a monotonically increasing load, the tension steel must first undergo a considerable amount of yielding. The actual point of failure shall be defined as that curvature, for which the strength drop reaches 25% of the yield moment(Fig 3). 2) Flexural failure due to fracture of tensile steel. The compression bars can buckle only after spalling of the concrete cover. Since it is rare that the concrete spalls off before the bars reach their yield strain, it is most likely that the buckling will follow immediately the spalling of the cover whereupon the capacity of the bars to carry compression forces drops rapidly.

## 4 Hysteretic Behavior of Reinforced Concrete

### 4.1 Basic Model Features

There are considerable differences between RC member behavior under monotonic and cyclic loading. As a result, failure modes that can be specifically excluded under monotonic load application, by following standard design and detailing procedures, may still prevail under cyclic loading. For example, bond failures can be avoided for most cases by properly developing the reinforcing bar forces. However, under repeated load reversals the steel-concrete interface can deteriorate rapidly and thus become the cause of failure.

A number of models have been proposed in the past to represent the hysteretic behavior of RC members. The Takeda-type model characterizes the hysteretic behavior more realistically than a bilinear or degrading bilinear formulation. The model of Roufaiel and Meyer(8) has been adopted herein, together with certain improvements to better represent stiffness and strength degradation, Fig 4. It is characterized by five different kinds of branches: 1) Elastic loading and unloading: $\Delta M = (EI)_1 \Delta \phi$. 2) Inelastic loading : If the moment exceeds the yield mement and is still increasing, the moment-curvature relationship is given by $\Delta M = (EI)_2 \Delta \phi$. 3) Inelastic unloading: If the moment decreases after the yield moment has been exceeded, the moment-curvature relationship becomes $\Delta M = (EI)_3 \Delta \phi$. 4) Inelastic reloading during closing of cracks: In a reversed load cycle, previously opened cracks tend to close, leading to an increase in stiffness and a characteristic "pinched" shape of the moment-curvature curve. $\Delta M = (EI)_4 \Delta \phi$. 5) Inelastic reloading after closing of cracks : Once the absolute value of the moment exceeds the "crack-closing moment", $Mp^+$ , and is still increasing, then the moment-curvature relationship is $\Delta M = (EI)_5 \Delta \phi$.

### 4.2 Stiffness Degradation

If the tensile reinforcement is strained beyond the yield point, then the bending stiffness drops from $(EI)_e$ to $p(EI)_e$, Fig 4, where "p" denotes the strain hardening ratio. Upon unloading, the bending stiffness is restored to a value somewhat less than the elastic stiffness, $(EI)_e$. The amount of stiffness degradation is proportional to the maximum displacement. To predict the bending stiffness associated with unloading from a curvature level $\phi$ (branch 3, Fig 4), one method is to employ a function of the form of $(EI)_3=(EI)_e(\delta / \delta_y)^{\beta}$, where $\beta$ is an empirical constant varying between 0.3 and 0.6, independent of the load history(5). Atalay and Penzien(1) used the expression $(EI)_3 = \alpha K_{cr}$ where $K_{cr} = (F_{max} / F_y)/(\delta_{max} / \delta_y)$ is the cracking stiffness, and $\alpha$ is a degradation factor and a function of absolute maximum displacement.

An alternative method is basically graphic. An auxiliary point($\phi_o^-$,$M_o^-$). is constructed as the point of intersection between a straight line of slope $p(EI)_e$ passing through the origin and a straight line of slope $(EI)_e$ passing through the point of minimum loading, ( $\phi_x^-$, $M_x^-$ ), Fig 4. The residual curvature associated with zero bending moment, $\phi_r^-$, is determined by connecting point ( $\phi_o^-$, $M_o^-$) with the point of actual maximum loading in the opposite direction, ( $\phi_x^+$, Mx'). It is debatable whether the slope of the above auxiliary line passing through the origin should be equal to $p(EI)_e$ as proposed by earlier investigators. According to Fig 4,

$$M_o^- = \frac{p}{1-p}(\phi_x^-(EI)_e - M_x^-), \qquad \phi_o^- = \frac{M_o^-}{p(EI)_e} \qquad \text{where } (\overline{EI})^+ = \frac{\overline{M}_x^+ - M_o^-}{\phi_x^+ - \phi_o^-}.$$

### 4.3 Shear Effect on Hysteretic Behavior

The effect of shear has been investigated by many researchers. When load reversal occurs within the inelastic range in the presence of high shear, the open shear cracks will initially permit the transfer of shear forces mostly through dowel action only, leading to a rather low stiffness. After the closing of such cracks, aggregate interlock and shear friction cause a significant increase of the member stiffness. Roufaiel(8) has modeled this effect by intoducing the"crack-closing" moment $M_p^+$, associated with curvature $\phi_p^+$, Fig 4.

The point $(M_p^+, \phi_p^+)$, can be determined as follows. The point $(M_p^+, \phi_p^+)$ is determined with the following coordinates (Fig 4):

$$\phi_n^+ = \phi_r - \frac{(\bar{EI})^+}{(\bar{EI})^+ - (EI)_e} \qquad M_n^+ = (EI)_e \phi_n^+$$

The coordinates of the crack-closing point can then be expressed as : $M_p = \alpha_p M_n^+$ and $\phi_p^+ = \alpha_p \phi_n^+$ where $\alpha_p = 0.4\ a/d - 0.6$, $\alpha_p = 0$ for $a/d \leq 1.5$ and $\alpha_p = 1$ for $a/d > 4.0$.

4.4 Strength Deterioration

In addition to stiffness degradation, RC members experience strength deterioration under cyclic loading beyond the yield level. The rate of strength deterioration and the failure curvature depend on many factors, such as the confinement ratio, axial force, concrete strength, etc. If the failure curvature for monotonic loading $\phi_f$, is known, it is possible to derive a strength deterioration curve.

Atalay and Penzien(1) had noticed some correlation between commencement of strength deterioration and the spalling of the concrete cover. But Hwang's experiments showed that strength deterioration can start at considerably lower load levels. Even for loads slightly above the yield level, damage and strength deterioration can be observed, provided a sufficiently large number of load cycles is applied. Roufaiel(8) found a strong correlation between the onset of strength deterioration and a "critical" displacement level, at which the concrete in the extreme compression fibre is strained to some limit value. But his investigation relied on test data with relatively small numbers of cycles for each load level, such as the test series by Ma et al(7). More significantly, it is unreasonable to stipulate such a precisely defined point of failure initiation, i.e. to say if this point is exceeded by a small amount, strength deterioration is initiated, but if it is missed by a small amount, no such strength deterioration takes place. Thus, Chung(3) suggested that strength deterioration is initiated as soon as the yield load level is exceeded, and the strength deterioration accelerates as the critical load level is reached. For this purpose, a strength drop index, $S_d$ , is proposed which defines the strength drop to be expected for a given curvature, $\phi$, in a single load cycle (Fig5). $\Delta M = S_d * M_f$, $S_d = [(\phi - \phi_y)/(\phi_f - \phi_y)]^w$ where $S_d$ = strength drop index for curvature in a single load cycle, $\Delta M$ = moment capacity reduction in a single load cycle up to curvature $\phi$, $\Delta M_f$ = moment capacity reduction in a single load cycle up to failure curvature $\phi_f$, $\phi_f$ =failure curvature corresponding to failure moment capacity $M_f$, $\omega$ = free constants. With $\Delta M$ denoting the strength drop in the ith subsequent load cycle for some curvature $\phi$, the residual strength after this load cycle is given by $m_i(\phi) = M(\phi) - i*\Delta M$. Where

$$\Delta M = [\ (\phi_f - \phi_y)p\ (EI)_e + M_y - M_f\ ] \left[ \frac{\phi - \phi_y}{\phi_f - \phi_y} \right]^w.$$

On the basis of selected experimental data, a value for $\omega$ of 1.5 appears to give good results.

## 5 Implementation and Numerical Examples

This hysteretic model has been also incorporated into the computer program, SARCF(Seismic Analysis of Reinforced Concrete Frames), which has been coded by chung(4). To illustrate the accuracy, with which the model can simulate hysteretic response of RC members, some numerical examples will be presented below. These cases were seletced from a number of simulation studies because they exhibited pronounced strength drops under constantamplitude loading, in which case the model's capacity to simulate strength deterioration is challenged most. For this purpose, Hwang's experiments(6) and some of the Berkeley tests(7) appeared to be most appropriate. To realistically simulate cyclic behavior of RC members, mathematical hysteretic models must consider the effect of strength deterioration, which can be clearly noticed in low cycle fatigue tests. Because of the phenomenon, eight experiments performed by Hwang and

Scribner(6) and two tests at the University at Berkeley(7) were selected for numerical simulation with the load histories shown in Table 1..

Hwang's experiments explored the relationship between load history and total energy dissipation capacity of RC flexural members. He tested a total of eleven cantilever specimens under displacement control and various load histories. All of these were analyzed, and agreement between experimental and analytical load deformation curves was excellent. Some of these numerical simulations are reproduced in Fig6. It is, in particular, noted how closely the experimentally observed strength deterioration is reproduced numerically. This is an indication that this hysteretic model promises to be reliable.

## 6. Conclusions

An analytic hysteretic model has been proposed with various enhancements that is believed to be more rational. It is based on a thorough investigation of the many factors that can contribute to the hysteresis of reinfored concrete member subjected to cyclic loadings. Some model parameters were calibrated against the few available experimental results. For example, the rate of strength deterioration and stiffness degradation were thus determined. An accurate reproduction of the experimental load-deformation curve is essential for meaningful nonlinear dynamic analysis of reinforced concrete structure. The principal shortcoming of the model is the small number of the test data which is based on the quasi-static experiment performed under the constant load amplitude. Thus, available experimental investigations be undertaken, especially to determine the relationship between load and deformation level and to study the influence of important parameters, such as confinement ratio, longitudinal steel reinforcement ratio, and shear reinforcement.

## 7.References


(1) Atalay, M, B. and Penzien, J., "The Seismic Behavior of Critical Regions of Reinforced Concrete Components as Influenced by Moment, Shear and Axial Forces," Report No. EERC-75-19, University of California at Berkeley, CA, 1975.

(2) Chung, Y. S., Meyer, C. and Shinozuka, M., "Seismic Damage Assessment of Reinforced Concrete Members," Report No. NCEER-87-0022, Nation Center for Earthquake Engineering Research, Buffalo, NY, October, 1987.

(3) Chung, Y. S., Meyer, C. and Shinozuka, M., "Modelling of Concrete Damage," ACI Structural Journal, Vol. 86 No. 3 May-June 1989.

(4) Chung, Y. S., Meyer, C. and Shinozuka, M., "SARCF User's Guide(Seismic Analysis of Reinforced Concrete Frames)," Report No. NCEER-88-0044, National Center for Earthquake Engineering Research, Buffalo, NY, November, 1988.

(5) Clough, R. W. and Johnston, S. B., "Effect of Stiffness Degradation on Earthquake Ductility Requirements," Proceeding of Japan Earthquake Engineering Symposium, October 1966.

(6) Hwang, T. H. and Scribner C. F., "R/C Members Cyclic Response During Various Loading," Journal of Structural Engeering, ASCE, Vol. 110, No.3, March 1984.

(7) Ma, S-Y. M., Bertero, V. V. and Popov, E. P., "Experimental and Analytical Studies on the Hysteretic Behavior of Reinforced Concrete Rectangular and T-Beam," ReportNo. EERC-76-2, University of California at Berkeley, CA, 1976.

(8) Roufaiel, M. S. L. and Meyer, C., "Analytical Modeling of Hysteretic Behavior of R/C Frames," Journal of Structural Engineering, ASCE, Vol. 113, NO. 3,March, 1987.

Table 1 Load Histories for Selected Test Specimens

| No | Basic Load Histories Pattern | Specimen | Figure No. | Investigator |
|---|---|---|---|---|
| 1 | 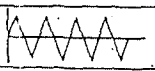 | S12<br>S22<br>S32 | 2.10<br>2.11 | Hwang and Scribner |
| 2 | 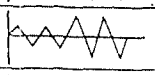 | S23<br>S33 | 2.12 | Hwang and Scribner |
| 3 | 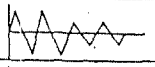 | S14<br>S24<br>S34 | 2.13 | Hwang and Scribner |
| 4 | 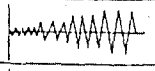 | R5 | 2.14 | Ma, Bertero and Popov |
| 5 |  | D35 | 2.15 | Popov, Bertero and Krawinkler |

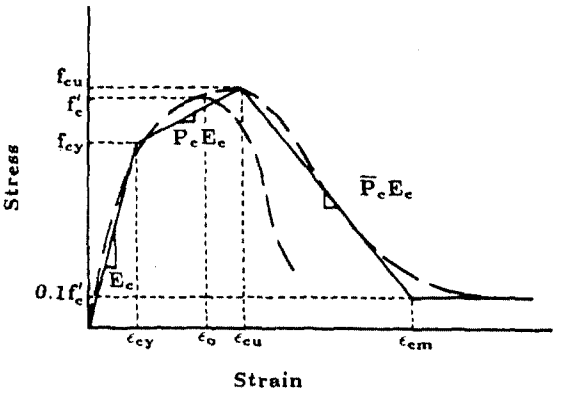


*Fig. 1*— Idealized Stress-Strain Curve of Concrete

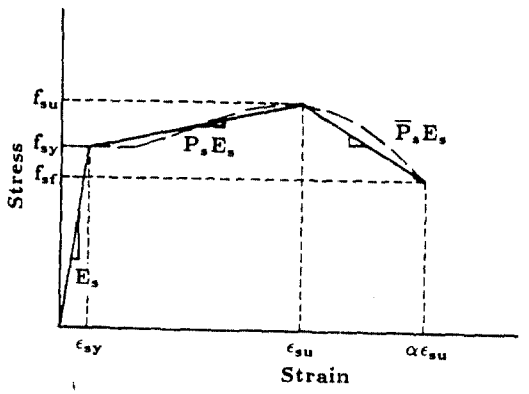


*Fig. 2*— Idealized Stress-Strain Curve of Tensile Steel

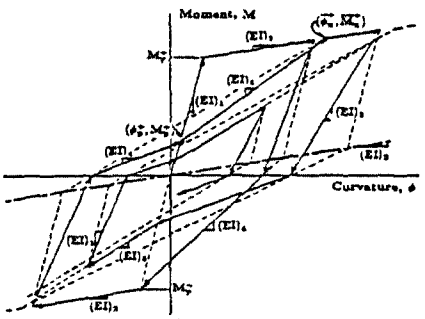


Fig. 4 – Typical Hysteretic Moment-Curvature Relationship

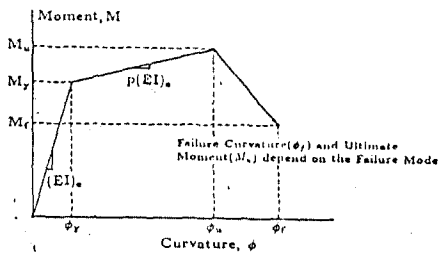


*Fig. 3*- Primary Moment - Curvature Curve

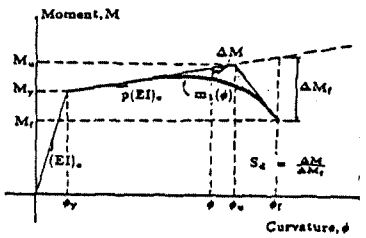


Fig. 5 – Strength Degradation Curve

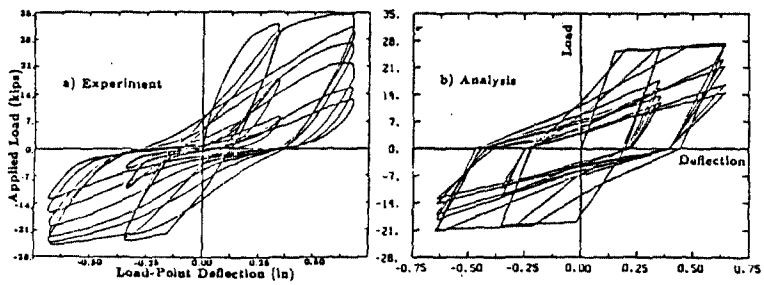


Fig. 6 – Experimental and Analytic Load-Deformation Curves for Beam S2-3 tested by Hwang